Article

JOURNAL OF THE CHINESE CHEMICAL SOCIETY

Catalytic Gas-phase Fluorination of Hexachlorobutadiene to 1,2-Dichlorotetrafluorocyclobutene over Cr/Zn-based Catalysts

Jinwei He,[a] Mengxue Zhang,[a] Biao Zhou[b] and Xiaomeng Zhou[c*]

[a]*The College of Environmental Science and Engineering, Nankai University, Tianjin 300071, China*
[b]*Faculty of Engineering, The University of Tokyo, Tokyo 113-8654, Japan*
[c]*Economics And Management College, Civil Aviation University of China, Tianjin 300300, China*

(Received: August 21, 2017; Accepted: December 28, 2017; DOI: 10.1002/jccs.201700274)

In this paper, the gas-phase fluorination of hexachlorobutadiene (HCBD) to synthesize 1,2-dichlorotetrafluorocyclobutene (DTB) was carried out over a series of Cr/M/Zn catalysts (M = Ni, Co, Cu, In, Al). The influence of prefluorination by different fluorinating agents (HF, 95%HF + 5%Cl_2, 95%HF + 5%O_2, CF_2O, CF_2Cl_2) on catalytic performance of Cr/Co/Zn sample was also investigated. The addition of prompters to the Cr/Zn catalyst improved remarkably its catalytic properties. The Cr/Ni/Zn catalyst exhibited the best catalytic activity (1.318 mmol/h/g) at 390 °C and the Cr/Co/Zn catalyst showed the best DTB selectivity (42.5%) at 350 °C. Compared to that of gaseous HF, the catalytic performance of the Cr/Co/Zn catalyst after treatment by HF + O_2 and CF_2O increased considerably, whereas for HF + Cl_2 and CF_2Cl_2 it showed little effect. In order to identify the different species (Cr—O, Cr—F, CrO_xF_y) present on catalysts' surface and determine their exact role, these catalysts before and after the reaction were characterized by X-ray photoelectron spectroscopy. It was found that the concentration of the various species was responsible for the activity and lifetime of catalysts. Moreover, a possible reaction route is proposed based upon the product distribution. The most feasible formation pathway of DTB proceeded via the cyclization of $C_4Cl_4F_2$ or $C_4Cl_3F_3$ to yield c-$C_4Cl_4F_2$ and c-$C_4Cl_3F_3$ followed by further the Cl/F exchange.

Keywords: Hexachlorobutadiene; 1,2-Dichlorotetrafluorocyclobutene; Catalytic fluorination; Promoters; Cr/Zn-based catalyst; Activation.

INTRODUCTION

1,1,1,4,4,4-Hexafluoro-2-butyne is widely used as an important fluorine-containing raw material. For example, hexafluoro-2-butyne is an established synthon for introducing two trifluoromethyl groups into furan or benzenoid systems.[1–4] Furthermore, 1,1,1,4,4,4-hexafluoro-2-butene, as a promising new-generation foaming agent due to its zero ozone depletion potential (ODP) value and a low global warming potential (GWP) value of 9.4,[5,6] also can be synthesized by catalytic hydrogenation of hexafluoro-2-butyne.[7,8] Thus, special attention has been paid to the manufacture of hexafluoro-2-butyne in the industry.

Several patents exist for the synthesis of hexafluoro-2-butyne.[9–11] Our research group proposed a three-step synthesis route for hexafluoro-2-butyne over a Cr-based catalyst (Scheme 1).[12] In the first step, 1,1,2,3,4,4-hexachloro-1,3-butadiene (HCBD) is catalytically converted to 1,2-dichloro-3,3,4,4-tetrafluorocyclobut-1-ene (DTB); in the second step, DTB is converted to 1.2,3,3,4,4-hexafluorocyclobut-1-ene; finally, hexafluoro-2-butyne is produced via the ring-opening reaction from hexafluorocyclobut-1-ene. Because HCBD is highly toxic and a persistent organic pollutant (POP), it was banned for use as a final product by the Stockholm Convention in 2013. The present route not only solves the persistent pollution problem of HCBD but also produces the versatile hexafluoro-2-butyne. However, the key to this method is the synthesis of DTB from HCBD (step 1).

*Corresponding author. Email: zhouxm@nankai.edu.cn

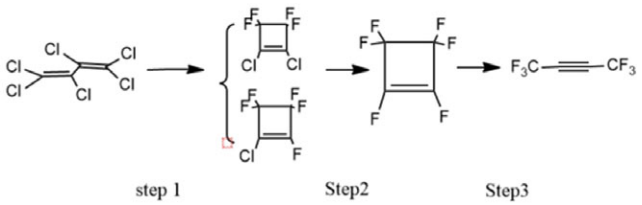

Scheme 1. Synthesis pathways for 1,1,1,4,4,4-hexafluoro-2-butyne.

Generally, the gas-phase fluorination with HF requires strong Lewis acid catalysts, notably chromium-based catalysts. Replacement of chlorines in chloroorganic materials (readily available from exhaustive chlorination of the parent organic compounds) by reaction with anhydrous HF in the presence of a Cr-based catalyst is the process widely employed for the preparation of fluorinated materials on a commercial scale. However, for the Cr-based catalyst to be active, it must have some specific properties. Cr-based catalysts in the presence of other elements such as Zn,[13] Ni,[14] In,[15] and Al[16] could improve their catalytic activities and inhibit side reactions. It has been established that a small amount of Zn added to chromium oxide can perturb HF adsorption, increase the dispersion of chromium, and lower the apparent activation energies involved in the Cl/F exchange to improve conversion and selectivity.[13,17]

On the other hand, many of catalytic fluorination reactions using metal oxides require activation with fluorinating agents.[18,19] Gas used for activation can result in structural and chemical changes and O/F exchange on the catalyst's surface, making it catalytically active. The most common method used for producing catalytically active materials involves the fluorination of Cr_2O_3 with HF. The purpose of prefluorination is that Cr_2O_3 can be converted into oxyfluoride (CrO_xF_y), which is believed to be the active sites for the reaction.[20]

In this study, various Cr/M/Zn precursors (M = Ni, Co, Cu, In, Al) were prepared via a precipitation method. HF gas was used to activate Cr/M/Zn samples (Ni, Cu, In, Al), and fluorinating agents (HF, HF + Cl_2, HF + O_2, CF_2O, CF_2Cl_2) were used to activate the Cr/Co/Zn samples. Catalytic performance of all catalysts was investigated through a series of experiments. Furthermore, these catalysts before and after the reaction were characterized by X-ray photoelectron spectroscopy (XPS), and an attempt to correlate the catalytic activity with the concentration of the different species present on the catalyst surface was made.

RESULTS AND DISCUSSION

Product distribution

Before studying the product distribution, the effects of various reaction conditions were investigated over the HF-Cr/Zn catalyst. The reaction temperature ranged from 200 to 410 °C and the residence time of DTB in the reactor from 4 to 20 s. The molar ratio of HF/HCBD was varied from 4 to 25. The experimental results showed that HCBD conversion and DTB selectivity were optimum when the molar ratio of HF/HCBD was 7:1, the residence time was 12 s, and the reaction temperature was kept at 310–390 °C. The obtained products were analyzed by GC-MS and ^{19}F NMR (Table 1). Besides the expected DTB, the other components obtained were $C_4F_3Cl_3$, $C_4F_2Cl_4$, and C_4FCl_5. $C_4F_3Cl_3$ has a cyclic structure, whereas $C_4F_2Cl_4$ and C_4FCl_5 are either linear or cyclic structures.

Table 2 presents the product distribution over the HF-Cr/Zn catalyst. The catalytic activity increased from 0.333 to 0.862 mmol/h/g when the reaction temperature was increased from 350 to 410 °C. However, the selectivity for DTB decreased from 10 to 5% when temperature was increased from 390 to 410 °C; also the selectivity for the other products changed significantly as the temperature was varied. So we believe that the reaction temperature can influence effectively the product distribution. A higher reaction temperature did not improve the conversion of the desired DTB; instead, it led to an increase of the other byproducts.

Catalytic performance

The fluorination of HCBD was carried out at 350–410 °C over HF-Cr/M/Zn catalyst or at 310–350 °C over Cr/Co/Zn catalyst after pretreatment by different fluorinating agents in order to compare their activities and identify the transformation products. The molar ratio of HF/HCBD was 7:1, and the residence time was 12 s.

The effect of various elements (Co, Ni, Al, In Cu) on the catalytic activity is presented in Table 3. It can be seen that the doping the HF-Cr/Zn catalyst with promoters was beneficial to the catalytic activity. The activity of the Cr/M/Zn catalysts varied from 0.361 to

Table 1. Product distribution

Products	Structure	MS peaks (*m/e*)	NMR chemical shifts
$C_4F_4Cl_2$		194[M^+],175[$M^+ - F$],159[$M^+ - Cl$], 125[$M^+ - Cl_2$],109[$M^+ - CF_2Cl$], 90[$M^+ - CF_2FCl$],74[$M^+ - CF_2Cl_2$].	$^{19}F(CF_2=)$-117.13 ppm
$C_4F_3Cl_3$		210[M^+],191[$M^+ - F$],175[$M^+ - Cl$], 156[$M^+ - FCl$],141[$M^+ - Cl_2$], 125[$M^+ - Cl_2F$],109 [$M^+ - CF_3Cl$], 90[$M^+ - Cl_3F$],71[$M^+ - CF_3Cl_2$].	$^{19}F(CF_2=)$-110.30 ppm, $^{19}F(CFCl=)$-117.64 ppm
$C_4F_2Cl_4$		228[M^+],191[$M^+ - Cl$], 174[$M^+ - FCl$],156[$M^+ - F_2Cl$], 141[$M^+ - CF_2Cl$],121[$M^+ - F_2Cl$], 106[$M^+ - CF_2Cl_2$],94[$M^+ - C_2F_2Cl_2$], 71[M^+- CF_2Cl_3],47[M^+- $C_3F_2Cl_3$]	–
C_4FCl_5		244[M^+],209[$M^+ - Cl$], 172[$M^+ - Cl_2$],141[$M^+ - CFCl_2$], 137[$M^+ - Cl_3$],102[$M^+ - Cl_4$], 90[$M^+ - CCl_4$],71[$M^+ - CFCl_4$], 66[$M^+ - C_3Cl_4$],47[$M^+ - C_3FCl_4$].	–
C_4Cl_6	CCl_2 = CCl-CCl = CCl_2	260[M^+],225[$M^+ - Cl$], 190[$M^+ - Cl_2$],153[$M^+ - Cl_3$], 141[$M^+ - CCl_3$],129[$M^+ - C_2Cl_3$], 118[$M^+ - Cl_4$],106[$M^+ - CCl_4$], 83[$M^+ - Cl_5$],71[$M^+ - CCl_5$], 57[$M^+ - C_2Cl_5$],47[$M^+ - C_3Cl_5$]	–

Table 2. Effect of reaction temperature on the product distribution over HF-Cr/Zn catalyst[a]

Temp. (°C)	Activity (mmol/h/g)	Selectivity (%)			
		DTB	$C_4F_3Cl_3$	$C_4F_2Cl_4$	Others
350	0.333	5	4	16	75
370	0.411	9	6	13	72
390	0.490	10	11	10	69
410	0.562	8	10	5	87

[a] Reaction conditions: HF/HCBD molar ratio of 7/1, residence time 12 s.

1.318/mmol/h/g and was higher than that of the Cr/Zn catalyst (0.333–0.562 mmol/h/g) at the same temperature. We presumed that the increased catalytic activity was related to the role of promoters. Indeed, the presence of promoters would modify the number of the active sites and the acid strength, which are favorable to the adsorption of the substrate. Again, the activity increased remarkably with the reaction temperature. This indicated that conversion of HCBD required a higher apparent activation energy. The increase of temperature significantly favored the transformation of HCBD. However, a higher reaction temperature does not mean better catalytic properties. In contrast, the activity of the Cr/Cu/Zn catalyst decreased from 0.671 to 0.596 mmol/h/g as temperature was increased from 370 to 410 °C, while that of Cr/Ni/Zn decreased from 1.318 to 1.264 mmol/h/g as temperature was increased from 390 to 410 °C. Comparing the various catalysts, Cr/Ni/Zn had the highest surface area of 78.2 m^2/g and exhibited the best catalytic activity (1.318 mmol/h/g) at 390 °C.

Table 4 shows the product distribution over different catalysts at a reaction temperature of 350 °C. These results show that product distribution is determined by the promoters. For Cr/Co/Zn and Cr/Ni/Zn catalysts, DTB was the main product under these reaction conditions and the selectivity to the former was 42.5% and that of the latter was 30.1%, while $C_4F_3Cl_3$ and $C_4F_2Cl_4$ were second most abundant products. For the Cr/Al/Zn sample, the DTB selectivity was zero, and for Cr/Cu/Zn and Cr/In/Zn catalysts the DTB selectivity was also unsatisfactory. In view of the above results, we believe that prompters can influence effectively the product distribution. Thus, to achieve high DTB

Table 3. Effect of promoters on the activity for transformation of HCBD (residence time 12 s, HF/HCBD = 7)

Tem. (°C)	Activity (mmol/h/g)				
	Cr/Co/ Zn (23.9 m^2/g)	Cr/Ni/ Zn (78.2 m^2/g)	Cr/Al/Zn (26.6 m^2/g)	Cr/In/ Zn (34.4 m^2/g)	Cr/Cu/Zn (63.2 m^2/g)
350	0.361	1.137	0.396	0.998	0.615
370	0.459	1.173	0.428	1.016	0.671
390	0.624	1.318	0.475	1.034	0.652
410	0.673	1.264	0.539	1.179	0.596

selectivity, the activity of Cr/Co/Zn catalyst pretreated by different fluorinating agents was also investigated.

Figure 1 shows catalytic activity and DTB selectivity over Cr/Co/Zn catalyst activated with different fluorinating agents and different temperatures. As seen from Figure 1(a), compared to gaseous HF, Cl_2 displayed only a small effect on the catalytic activity in the fluorination of DTB. However, the activities of O_2-Cr/Co/Zn and CF_2O-Cr/Co/Zn catalysts were higher than that of the HF-Cr/Co/Zn catalyst. For CCl_2F_2-Cr/Co/Zn catalyst, the activity and DTB selectivity were better than with HF-Cr/Co/Zn at the reaction temperatures of 310 and 350 °C; nevertheless, a significant decrease could be noticed when temperature was 330 °C. For other catalysts, the selectivity of DTB decreased in the order O_2-Cr/Co/Zn > HF-Cr/Co/Zn > Cl_2-Cr/Co/Zn > CF_2O-Cr/Co/Zn.

Characterization of the various catalysts by XPS

In order to identify the different species present on the catalyst surface and try to understand the exact roles of the doping agent and fluorinating agents, the catalysts were characterized by XPS. We attempted also to correlate the catalytic properties with the concentrations of the different species present on the catalyst surface.

Table 4. Product distribution at the reaction temperature of 350 °C

Sample	Selectivity (%)		
	DTB	$C_4F_3Cl_3$	$C_4F_2Cl_4$
HF-Cr/Co/Zn	42.5	25	10
HF-Cr/Ni/Zn	30.1	15.8	15.8
HF-Cr/Al/Zn	0	19.2	23.1
HF-Cr/In/Zn	3.6	7.2	11.0
HF-Cr/Cu/Zn	9.1	15.1	18.2

Figures 2 and 3 show the XPS spectra of Cr 2p and Zn 2p levels for the HF-Cr/Zn catalyst, respectively, both before and after the reaction. As shown in Figure 2, before the reaction, the Cr $2p_{3/2}$ peak was

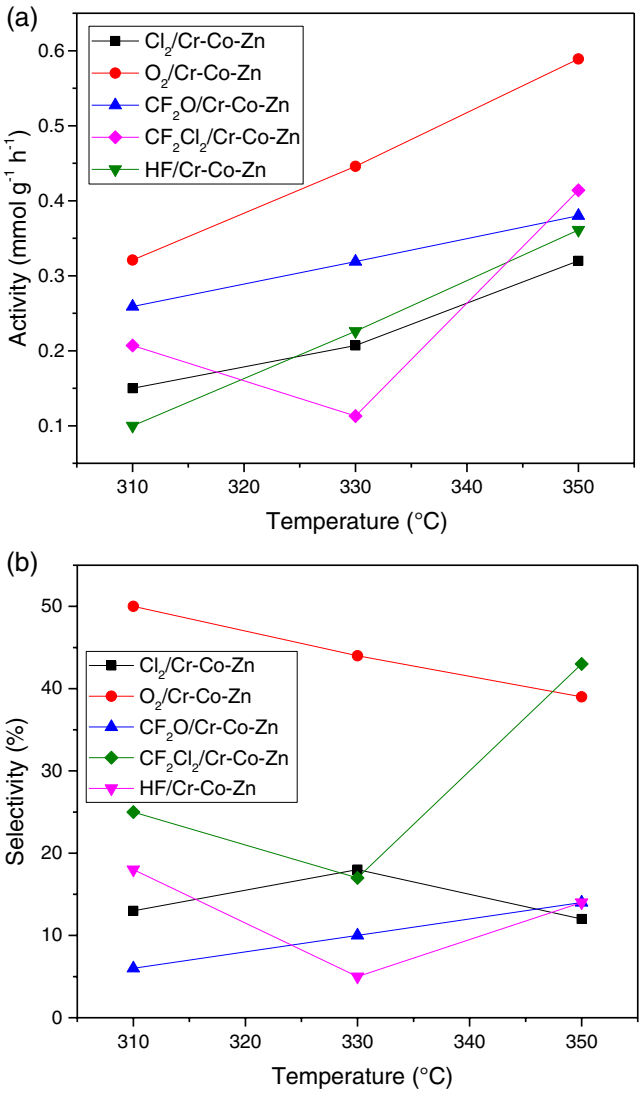

Fig. 1. Catalytic activity (a) and DTB selectivity (b) over Cr/Co/Zn catalysts.

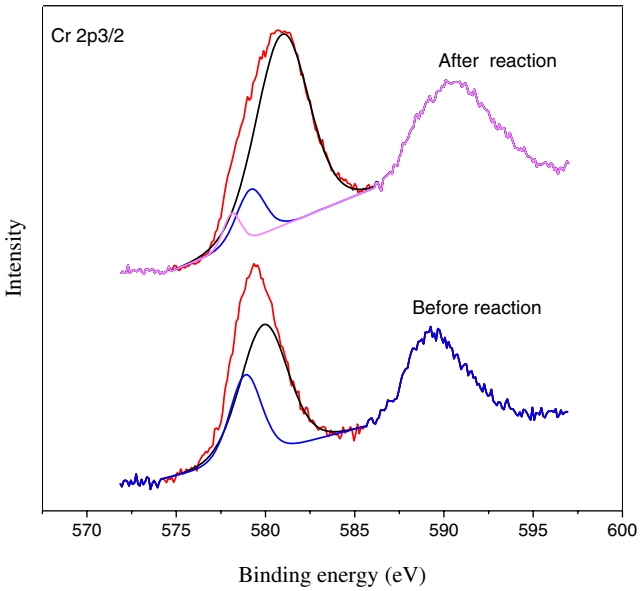

Fig. 2. XPS spectra of the Cr 2p level for HF-Cr/Zn catalysts before and after reaction.

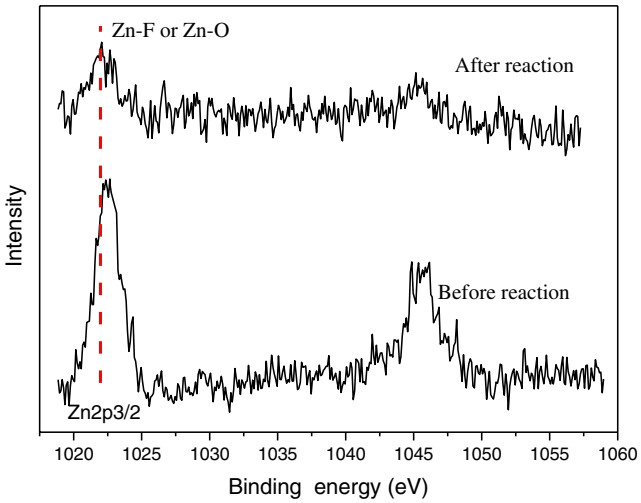

Fig. 3. XPS spectra of the Zn 2p level for HF-Cr/Zn catalysts before and after reaction.

resolved into two components at 578.4 and 580.4 eV. The prominent peak at 580.4 eV can be assigned to the Cr—F bond in CrF_3-like species,[21] and the peak at 578.4 eV could be attributed to the Cr—O bond in the structure corresponding to Cr_2O_3.[22] Then, after the reaction, the spectrum of Cr 2p became broadened and was shifted to higher binding energy. The broad Cr $2p_{3/2}$ peak of the Cr/Zn sample was deconvoluted to three components at 578.9, 581.7 and 584.6 eV, respectively. Two kinds of Cr species could be attributed to Cr-O (578.4 eV) in Cr_2O_3 and Cr-F (580.4 eV) in CrF_3, respectively. Thus, the 579.1 eV binding energy may assigned to CrOF in the CrO_xF_y structure.[17] Before the reaction, the Zn $2p_{3/2}$ spectrum of the HF-Cr/Zn catalysts indicated the presence of a single species with a binding energy of 1022.3 eV, which could be attributed to ZnF_2 or ZnO (Figure 3). After the reaction, the Zn $2p_{3/2}$ spectrum of the samples exhibited only a blurred peak. These results indicated that the catalysts had strongly interacted with reactants during the reaction process, which resulted in extensive change of the chemical environments of the Cr and Zn atoms.

The F 1s and O 1s core-level spectra of Cr/Zn catalysts before and after reaction further confirmed the above results (Figure 4). As shown in Figure 4(a), the F 1s peak was resolved into two components at 685.1 and 687.5 eV. Before the reaction, the prominent peak at 685.1 eV could be assigned to Cr-F in CrF_3 or Zn-F in ZnF_2.[23] After the reaction, the concentration of the another species Cr-F (687.5 eV) in CrO_xF_y increased.[24] A similar trend in the F 1s profiles (Figure 4(b)) could also be noted. The O 1s spectrum was fitted by two components at 531.4 and 533.4 eV, respectively. Chung *et al.*[25] reported the binding energies of 531.4 and 533.4 eV for Cr-O and CrOF, respectively. We therefore assigned the peak located at the higher binding energy to CrOF and that at the lower binding energy to Cr-O.

The quantification of the intensities of the bands corresponding to the different species on the HF-Cr/Zn catalyst surface is reported in Table 5. The content of the surface species is calculated by the peak area of the species divided by the total peak area of all species. A change in the distribution of three species (Cr-O, Cr-F, and CrOF) is noticed before and after the reaction. For the Cr 2p species, before reaction the contents of Cr-F, Cr-O, and CrOF are 69.96, 30.04, 0%, respectively. For the spent catalyst, the contents of Cr-F, Cr-O, and CrOF are 83.87, 4.72, and 11.4%, respectively. This suggests that the concentration of the species designated as Cr-O decreased after the reaction, whereas the concentration of the species CrOF and Cr-F increased, which may be due to the fact that a few CrO or Cr-F species are converted to CrOF on the catalyst surface during the reaction process. It has been well recognized that the presence of CrO_xF_y species is disadvantageous

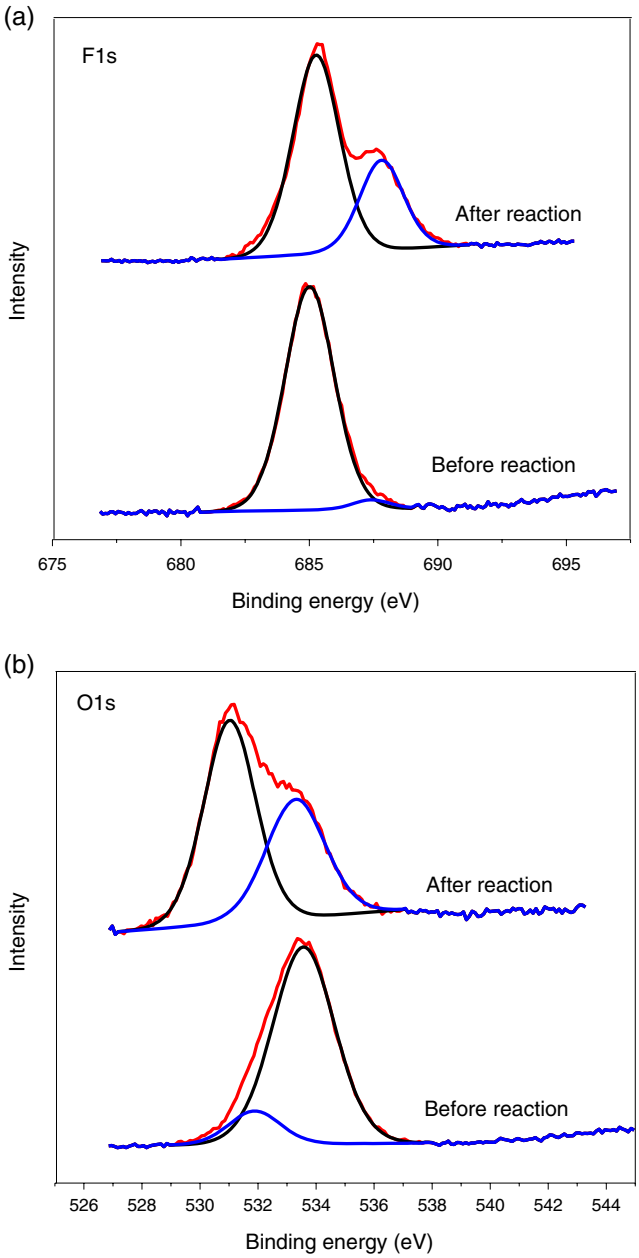

Fig. 4. XPS spectra of (a) the F 1s and (b) the O 1s of HF-Cr/Zn catalysts before and after reaction.

to the Cl/F exchange reactions.[26] The time-on-stream of the HF-Cr/Zn catalyst was assessed. After the reaction, the catalytic activity decreased compared to the initial value. Thus, we guess that the decline in activity is due to the increase of the CrOF species on the catalyst surface. There was a decline in the mol% ratio of Cr-F/CrOF (from 32.0 to 2.4) in the F 1s and Cr-O/CrOF (from 6.8 to 1.5) in the O 1s spectrum after the reaction.

Table 5. Amounts of the different species on the catalyst surface determined from XPS data for HF-Cr/Zn catalysts before and after reaction

Elements	Species	Binding energy (eV)±0.1	mol %	
			Before	After
Cr	Cr-F	580.4	69.96	83.87
	Cr-O	578.4	30.04	4.72
	CrOF	579.1	0	11.4
F	Cr-F or Zn-F	685.1	96.97	70.26
	CrFO	687.5	3.03	29.74
O	Cr-O	531.4	87.71	60.08
	CrOF	533.4	12.29	39.92

This further confirmed the increase of CrOF and Cr-F species and decrease of Cr-O species after the reaction.

In order to determine the impact of promoters on the surface properties of Cr/Zn catalyst, the XPS spectra of different HF-Cr/M/Zn samples before the reaction were investigated. As shown in Figure 5, the Cr 2p profiles are similar for HF-Cr/Zn, HF-Cr/Ni/Zn, HF-Cr/Cu/Zn, and HF-Cr/In/Zn catalysts. However, a shift toward lower binding energy of the Cr $2p_{3/2}$ peak is observed after the addition of promoters Ni, Cu, and In, which can be attributed to the increase in the number of the Cr-O species. In contrast, the core peak of Cr

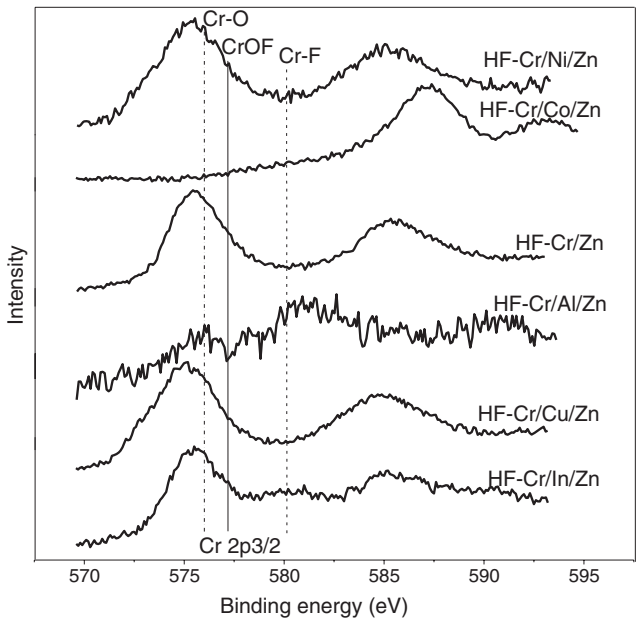

Fig. 5. XPS spectra of the Cr 2p of HF-Cr/M/Zn catalysts before reaction.

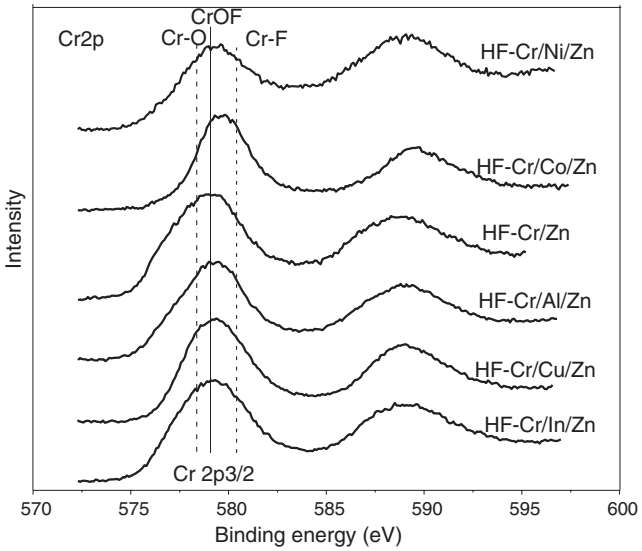

Fig. 6. XPS spectra of the Cr 2p of HF-Cr/M/Zn catalysts after reaction.

$2p_{3/2}$ shifted to the high-energy side after introducing Co onto the Cr/Zn sample. For the HF-Cr/Al/Zn catalyst, the Cr 2p spectrum hardly exhibited any peak. It was reported that the reaction between Al_2O_3 with HF to form AlF_3 required a lower reaction enthalpy value. So the formation of AlF_3 resulted in the disappearance of the Cr 2p peak. This trend of the change in promoters upon HF-Cr/Zn catalyst is also confirmed in the O 1s and F 1s core-level spectra of these samples (not shown here). As mentioned above, catalytic activity is related to the presence of promoters on the Cr/Zn catalyst. Therefore, the role of different dopants can be ascribed to the difference in distribution of active Cr species on the catalyst. Thus, it can be concluded that dispersed CrOF species are mainly responsible for the DTB selectivity and that Cr-O is crucial to achieve this high activity. The difference in the contents of the surface CrOF and Cr–O species coincided exactly with the catalytic behaviors of the various catalysts

The XPS spectra of HF-Cr/M/Zn samples after the reaction were also studied to reveal the deactivation of catalysts (Figure 6). After the reaction, the Cr 2p profiles were similar for all samples. This suggests that all samples underwent a decline in activity during the reaction. Table 6 gives the results of the XPS analysis of the various elements on the surface of HF-Cr/M/Zn catalysts before and after the reaction. A change in the distribution of the various elements is noticed depending on the dopants before and after the reaction. Before the reaction, the molar content of Cr element decreased in the order HF-Cr/Co/Zn > HF-Cr/Cu/Zn > HF-Cr/Ni/Zn > HF-Cr/In/Zn > HF-Cr/Al/Zn. In contrast, the molar content of Cr element decreased in the order HF-Cr/Al/Zn > HF-Cr/Ni/Zn > HF-Cr/In/Zn > HF-Cr/Cu/Zn > HF-Cr/Co/Zn after the reaction. The mol % of Cr was found to be predominant before the reaction, whereas the mol% of O and F were predominant after the reaction.

Figure 7 shows the XPS spectra of the Cr 2p level for various Cr/Co/Zn catalysts fluorinated by different fluorinating agents. The Cr 2p profiles are similar for HF-Cr/Co/Zn and CF_2O-Cr/Co/Zn samples. However, a slight shrinking of Cr 2p line can be observed. The fluorinating agent CF_2Cl_2 has a remarkable effect on Cr 2p of the Cr/Co/Zn catalyst, and the double peaks of the Cr 2p shifted to a single peak. After treatment by

Table 6. Relative molar contents of different elements on the HF-Cr/M/Zn catalysts before and after reaction

		Molar content (%)					
Sample		Cr	F	O	Zn	M	Cl
HF-Cr/Co/Zn	Before	13.27	34.23	50.95	1.55	0	0
	After	10.4	55.91	31	0.56	0	2.49
HF-Cr/Ni/Zn	Before	10.4	19.87	66.32	1.66	1.1	0.64
	After	20.37	39.72	34.24	1.82	0	3.85
HF-Cr/Al/Zn	Before	2.34	11.67	84.85	1.14	0	0
	After	24.22	54.3	16	1.41	1.29	2.77
HF-Cr/In/Zn	Before	7.92	26.33	62.23	1.87	0.8	0.74
	After	18.86	39.59	37.75	0.86	0.78	2.15
HF-Cr/Cu/Zn	Before	13.16	25.76	58.15	1.57	0.91	0.46
	After	18.53	36.1	39.22	0.75	0.99	4.41

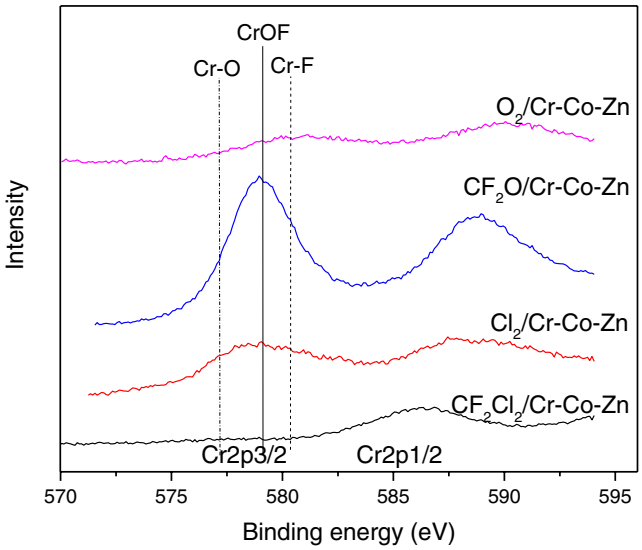

Fig. 7. XPS spectra of Cr 2p for Cr/Co/Zn catalyst activation by different fluorinating agents.

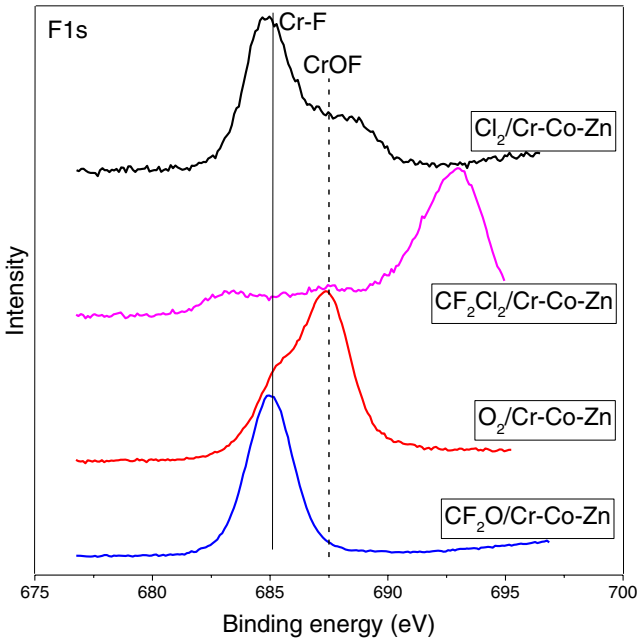

Fig. 8. XPS spectra of F 1s for Cr/Co/Zn catalysts.

O_2 and Cl_2, the spectrum of Cr 2p became broad and was shifted to a higher binding energy. These results indicated that Cr/Co/Zn precursor strongly interacted with various fluorinating agents during the prefluorination process, leading to extensive change of the chemical environment of the Cr atom.

From the XPS measurements shown in Figure 8, two peaks having the F 1s binding energy of 685.1 and 687.5 eV can be identified. We assigned the peak located at the higher binding energy to CrOF and that at the lower binding energy to Cr-F. Cr-F was found to be dominating in the Cl_2-Cr/Co/Zn catalyst and CrOF was dominating in the O_2-Cr/Co/Zn catalyst. CF_2O gas treatment of the Cr/Co/Zn precursor generated only the Cr-F species. In contrast, the fluorinating agent CF_2Cl_2 gave neither CrOF nor Cr-F species but generated a different species with a higher binding energy of 693.1 eV.

The influence of prefluorination by different fluorinating agents over Cr/Co/Zn catalysts on the amount of fluorine (or oxygen) can be determined from the variations of the ratios I_F/I_{Cr} (or I_O/I_{Cr}) and $I_F/I_{(Cr + Co + Zn)}$ (or $I_O/I_{(Cr + Co + Zn)}$) (Figure 9), where I is the intensity of a peak in the wide XPS spectra. The ratios I_O/I_{Cr} and $I_O/I_{(Cr + Co + Zn)}$ decreased in the order HF > Cl_2 > CF_2O > CF_2Cl_2 > O_2 and HF > CF_2Cl_2 > Cl_2 > CF_2O > O_2, respectively. The ratios I_F/I_{Cr} and $I_F/I_{(Cr + Co + Zn)}$ decreased in the order O_2 > CF_2O > CF_2Cl_2 > Cl_2 > HF and O_2 > CF_2Cl_2 > CF_2O > Cl_2 > HF, respectively. The results showed that after the treatment by O_2 the Cr/Co/Zn precursor was more easily fluorinated.

Possible reaction path

A simplified reaction path from HCBD to DTB was proposed based on experimental results with theoretical calculations by our research group (Figure 10).[27]

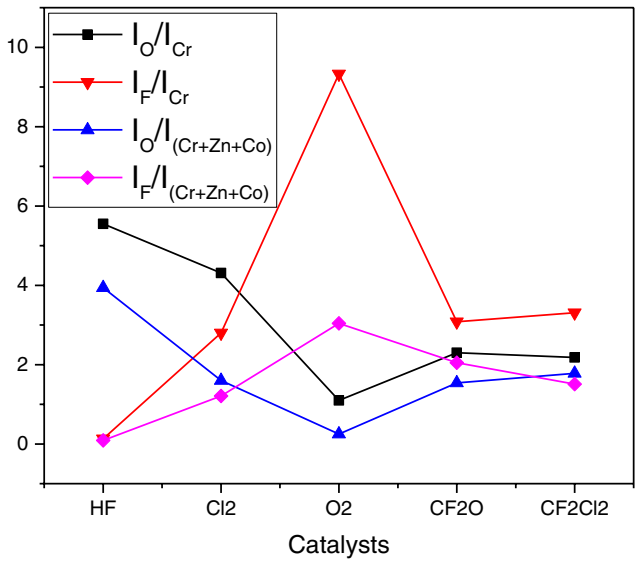

Fig. 9. Elements molar ratios over Cr/Co/Zn catalysts.

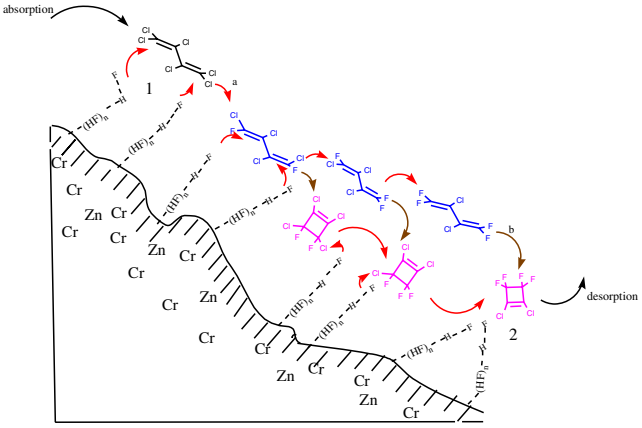

Fig. 10. Possible reaction paths for the fluorination of HCBD catalyzed by Cr/M/Zn catalysts.

In general, HCBD is stable with no self-cyclization reaction even at 500 °C.[28] On the contrary, HCDB was found in the products when hexachlorocyclobutene was heated to 195 °C.[29] These results validated that the F/Cl exchange reaction takes place prior to the cyclization of HCBD. In addition, NMR analyses showed that the Cl/F exchange primarily occurred at the terminal CCl_2 groups rather than at the inner CCl groups. Hence, by comparing the product distribution, the transformation of HCBD to BTB may involve a Cl/F exchange reaction forming $C_4Cl_4F_2$ first; and then, $C_4Cl_4F_2$ would proceed either via a cyclization forming c-$C_4Cl_4F_2$ followed by further Cl/F exchange reactions, or via a Cl/F exchange reaction forming $C_4Cl_3F_3$ and $C_4Cl_2F_4$ followed by further cyclization.

EXPERIMENTAL

Chemicals

1,1,2,3,4,4-Hexachloro-1,3-butadiene (HCBD) (98%) was obtained from Letai Chemical Industry Co., Ltd. (Tianjin, China). Anhydrous HF (AHF) (>99.9%), Cl_2 (>99.9%), O_2 (>99.9%), CF_2O (>99.9%), CF_2Cl_2 (>99.9%), and N_2 (>99.9%) were purchased from Beijing North Oxygen Specialty Gases Institute Co., Ltd. (Beijing, China). $NH_3{\cdot}H_2O$ (30%) was obtained from Beijing Chemical Works Co., Ltd. (Beijing, China). Analytical-grade $CrCl_3{\cdot}6H_2O$ (>99%), $Zn(NO_3)_2{\cdot}6H_2O$ (>99%), $Ni(NO_3)_2{\cdot}6H_2O$ (>99%), $Cu(NO_3)_2$ (>99%), $In(NO_3)_3{\cdot}5H_2O$ (>99%), $Al(NO_3)_3{\cdot}9H_2O$(>99%), and $Co(NO_3)_2{\cdot}6H_2O$(>99%) were purchased from Xilong Chemical Co., Ltd. (Guangxi, China).

Preparation of the catalyst

The Cr/M/Zn precursors were prepared via a coprecipitation method. The molar ratio of Cr, Zn, and M (Ni, Cu, In, Al, Co) was 85:10:5 in the precursor. Analytical-grade $CrCl_3$, $M(NO_3)_x$, and $Zn(NO_3)_2$ were first dissolved in distilled water. A hydroxide was obtained from 246 g of a 10% $CrCl_3$ solution. Then 30% $NH_3{\cdot}H_2O$ was added to the above prepared solution under continuous stirring until a precipitated slurry was obtained. Subsequently, the resulting slurry was filtered, washed with deionized water several times, and baked at 110 °C for 24 h in a drying oven. Finally, the dried solid was ground, mixed with 2 wt% graphite, and pelleted into cylindrical wafers (diameter = 2 mm; height (h) = 3 mm). The Cr/M/Zn precursors were formed by calcining the pellets at both 250 °C for 10 h and at 400 °C for 10 h under a N_2 flow rate of 150 mL/min.

Prior to the reaction, pretreatment was carried out to activate the precursors with different fluorinating agents (HF, 95%HF + 5%Cl_2, 95%HF + 5%O_2, CF_2O, CF_2Cl_2). Twenty grams of the precursors was packed into the reactor. A mixture of N_2 (100 mL/min) and the fluorinating agent (50 mL/min) was passed through reactor at 150 °C for 10 h. Then, the N_2 flow rate was decreased to 50 mL/min and the fluorinating agent flow rate was increased to 100 mL/min at 250 °C for 10 h. Subsequently, the N_2 flow was stopped and the sample was heated at 400 °C for 10 h in the fluorinating agent at a flow rate of 150 mL/min. Finally, the pretreated catalysts, which were denoted as HF-Cr/M/Zn, Cl_2-Cr/M/Zn, O_2-Cr/M/Zn, CF_2O-Cr/M/Zn, and CF_2Cl_2-Cr/M/Zn, respectively, were formed.

Reaction conditions

Catalytic activity measurements for the fluorination of HCBD were carried out in a fixed-bed reactor. Twenty grams of the catalyst was placed in the reactor. Then HCBD and HF, converted to the vapor-phase in a vaporizer at 230 °C, were passed together into the stainless steel reactor at 310–410 °C with a contact time of 12 s. The molar ratio of HF:HCBD was 7:1. HCBD was dosed via a Masterflex metering pump, and HF was dosed using a mass flow controller. The products were cooled with an ice bath and collected. The collected products were washed in a 60 °C warm water stream to remove HF and HCl, and dried successively

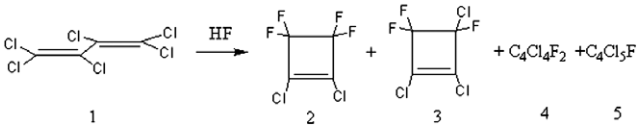

Scheme 2. Reaction products for the reaction of HCBD with HF.

with anhydrous sodium sulfate and molecular sieves (4 Å). The obtained products were analyzed by GC, GC-MS, and ^{19}F NMR. As shown in Scheme 2, the reaction of HCBD with HF in the presence of catalysts yielded main products DTB, $C_4Cl_3F_3$, $C_4Cl_4F_2$, and C_4Cl_5F.

The catalytic activity A (mmol/h/g) was defined as the conversion multiplied by the flow of HCBD (mol/h) and divided by the mass of catalyst.

Characterization

Gas chromatography-mass spectroscopy (GC-MS) was carried out on a Shimadzu-QP 2010 Ultra series system, which was equipped with a jet separator for the 2010 GC. The capillary column (Model DB-5, J&W Scientific, Inc.) had an inner diameter (i.d.) of 0.25 mm and a length of 30 m.

Gas chromatography (GC) was carried out under the following operating conditions: capillary column 0.25 mm i.d. and 30 m length (DB-5, J&W Scientific, Inc.); column temperature maintained at 35 °C for 3 min and then heated to 200 °C at the rate of 10 °C/min and held at that temperature for 3 min; the injector and detector temperatures set at 280 and 200 °C, respectively; split ratio 80:1; and sample volume 0.1 μL.

^{19}F NMR spectra were recorded on a Bruker AV400 instrument at 400 MHz with $CFCl_3$ as the internal standard.

The adsorption–desorption isotherm of nitrogen was measured by a Micromeritics ASAP 2020 automated gas sorption system at −196 °C after the sample was degassed under vacuum at 300 °C for 3 h. The specific surface areas of all samples were calculated by the Brunauer–Emmett–Teller (BET) method, and the average pore diameters were determined by the Barrett–Joyner–Halenda (BJH) method

XPS measurements were carried out on a Kratos Axis Ultra DLD Multitechnique X-ray photoelectron spectrometer (UK) equipped with a monochromatic Al Kα X-ray source (hυ = 1486.6 eV). All XPS spectra were recorded using an aperture slot measuring 300 μm × 700 μm. Survey and high-resolution spectra were recorded with pass energies of 160 and 40 eV, respectively. Accurate binding energies (within ±0.2 eV) were determined with respect to the position of the adventitious C 1s peak at 284.6 eV

CONCLUSIONS

Reaction conditions for the fluorination of HCBD catalyzed by Cr/M/Zn catalysts were investigated. The catalytic activity of the Cr/Zn-based catalyst was improved by the addition of small amounts of prompters. The Cr/Ni/Zn catalyst exhibited better catalytic activity, but the DTB selectivity was unsatisfactory. However, the Cr/Co/Zn catalyst improved greatly the DTB selectivity. Subsequently, different fluorinating agents (HF + Cl_2, HF + O_2, CF_2O, CF_2Cl_2) were used to fluorinate the Cr/Co/Zn precursor. After treatment by HF + O_2, the catalytic performance increased remarkably. Characterization by means of XPS spectra revealed that promoters and the activation period of Cr/M/Zn samples before and after the reaction involved changes in the different species. Furthermore, a possible reaction path was proposed.

ACKNOWLEDGMENTS

This work was supported by the National Natural Science Foundation of China (Grant No. 51176078) and the Special Project of the Basic Work of Science and Technology Police of MPS (Grant No. 2016GABJC35).

REFERENCES

1. C. D. Wei, *J. Org. Chem.* **1962**, *27*(3693), 3344.
2. A. Abubakar, B. Booth, A. Tipping, *J. Fluorine Chem.* **1991**, *55*, 189.
3. H. N. C. Wong, *Synthesis* **1984**, *1984*, 787.
4. A. Abubakar, B. Booth, N. Suliman, A. Tipping, *J. Fluorine Chem.* **1992**, *56*, 359.
5. M. J. Molina, F. S. Rowland, *Nature* **1974**, *249*, 810.
6. Q. Fu, X. G. Sun, S. J. Xiang, X. L. Kong, *Organo-Fluorine Ind.* **2012**, *1*, 30.
7. A. L. Henne, G. A. William, *J. Chem. Soc.* **1949**, *71*, 298.
8. R. N. Haszeldine, *J. Chem. Soc.* **1952**, *473*, 2504.
9. C. E. Frank, A. U. Blackham, *J. Am. Chem. Soc.* **1950**, *72*, 3283.
10. W. R. Hasek, W. C. Smith, V. A. Engelhardt, *J. Am. Chem. Soc.* **1960**, *82*, 543.
11. A. L. Henne, P. Trott, *J. Am. Chem. Soc.* **1947**, *69*, 1820.

12. M. L. Zhang, Z. Yao, B. Zhou, A Method of Synthesizing hexafluoro-2-butadiene. China Patent CN105348034A, **2015**.
13. D. W. Bonniface, J. D. Scott, M. J. Watson, J. R. Fryer, P. Landon, W. D. S. Scott, G. Webb, J. M. Winfield, *Green Chem.* **1999**, *1*, 9.
14. B. Cheminal, F. Garcia, E. Lacroix, A. Lantzk, Mass Catalysts Based on Chromium and Nickel Oxides and their Application to the Fluorination of Halogenated Hydrocarbons. US Patent 5,523,500, **1996**.
15. J. K. Murthy, U. Groß, S. Rüdiger, E. Ünveren, E. Kemnitz, *J. Fluorine Chem.* **2004**, *125*, 937.
16. M. Subramanian, *Science* **2002**, *297*, 1665.
17. A. Loustaunau, R. Fayolle-Romelaer, S. Celerier, A. D. Huysser, L. Gengembre, S. Brunet, *Catal. Lett.* **2010**, *138*, 215.
18. G. B. McVicker, C. J. Kim, J. J. Eggert, *J. Catal.* **1983**, *80*, 315.
19. R. I. Hegde, M. A. Barteau, *J. Catal.* **1989**, *120*, 387.
20. D. H. Cho, Y. G. Kim, M. J. Chung, J. S. Chung, *Appl. Catal. B* **1998**, *18*, 251.
21. E. Kemnitz, A. Kohne, I. Grohmann, A. Lippitz, *J. Catal.* **1996**, *159*, 270.
22. A. Cimono, B. A. De Angelis, A. Luchetti, G. Minelli, *J. Catal.* **1976**, *45*, 316.
23. S. Brunet, B. Requieme, E. Colnay, J. Barrault, M. Blanchard, *Appl. Catal. B* **1995**, *5*, 305.
24. W. Mao, L. Kou, B. Wang, Y. Bai, W. Wang, J. Lu, *Appl. Catal. A* **2015**, *491*, 37.
25. Y. S. Chung, H. Lee, H. D. Jeong, Y. K. Kim, H. G. Lee, H. S. Kim, S. Kim, *J. Catal.* **1998**, *175*, 220.
26. B. Adamczyk, O. Boese, N. Weiher, S. L. M. Schroeder, E. Kemnitz, *J. Fluorine Chem.* **2000**, *101*, 239.
27. A. P. Scott, L. Radom, *J. Phys. Chem.* **1996**, *100*, 16502.

